Ab initio lattice dynamics of diamond

P. Pavone, K. Karch, O. Schütt, W. Windl, and D. Strauch
Institut für Theoretische Physik der Universität Regensburg, Universitätsstrasse 31, D-8400 Regensburg, Germany

P. Giannozzi
Scuola Normale Superiore, Piazza dei Cavalieri 7, I-56100 Pisa, Italy

S. Baroni
Scuola Internazionale Superiore di Studi Avanzati-International School for Advanced Studies (SISSA-ISAS), via Beirut 4, I-34014 Trieste, Italy

(Received 16 March 1993)

We present a first principles calculation of lattice dynamical properties of diamond. Our calculations have been performed using density-functional perturbation theory together with plane-wave expansion and nonlocal pseudopotentials. As a first step we have evaluated the equilibrium structure of diamond via the minimization of the total energy. Then, harmonic phonon dispersion curves and phonon eigenvectors have been evaluated within the linear-response framework. As a by-product of the calculation we have also obtained the internal-strain parameter. Furthermore, we have also tested the validity of the *ab initio* calculation for describing properties beyond the harmonic approximation. Using the quasiharmonic approximation we have calculated the thermal expansion coefficient and the mode Grüneisen parameter dispersion curves. Where experimental data are available, good agreement is found with our theoretical predictions.

I. INTRODUCTION

The lattice static and dynamical properties of diamond differ substantially from those of the other group-IV tetrahedral semiconductors. Several distinctive features, such as small lattice parameter, large bulk modulus, and cohesive energy,[1] characterize the equilibrium properties of diamond with respect to Si and Ge in the same structure. Also the electronic properties of diamond are very peculiar. The presence of a relevant double-hump feature[2] in the ground-state electron density along the bonds is something really unusual within the class of monoatomic tetrahedral semiconductors.

Large differences also arise considering lattice dynamical properties such as the phonon dispersion curves and the thermal expansion. The typical flatness of the transverse acoustic branches in large regions close to the boundaries of the Brillouin zone (BZ), which characterizes the other group-IV elemental semiconductors, is completely lacking in diamond. Furthermore, relevant features of the phonon dispersion of diamond, e.g., the behavior of the uppermost phonon branch in the vicinity of the Γ point, have been experimentally investigated, however, with insufficient resolution and/or statistics.[3,4] Finally, the thermal expansion coefficient of diamond does not show the characteristic negative behavior in the low-temperature limit which is found for the other group-IV elemental crystals.[5]

All these facts have attracted general interest. Our specific purpose is to give a detailed description of lattice dynamical properties of diamond using a parameter-free quantum mechanical description. During the last years, two different approaches have been developed to achieve a microscopic description of lattice dynamics from first principles: the frozen phonon method[6] and the density-response or dielectric theory.[7]

In the frozen phonon approach, the electronic ground-state energy is calculated as a function of the atomic positions. Then, lattice dynamical properties are derived by comparing the energy corresponding to different displacement patterns. In principle, any phonon property with a wave vector commensurate with a reciprocal-lattice vector can be studied. However, because of the increase of computational effort caused by the use of large supercells, one can deal only with perturbations for wave vectors along high-symmetry directions. Direct applications of this approach to diamond were successful in order to get results such as the optical-phonon frequency at the Γ point,[8] elastic properties,[9,10] and anharmonic phonon coupling.[11]

On the other hand, in the density-response theory no restriction is imposed on the wave vector of the perturbation. However, this approach involves explicit knowledge of the inverse dielectric function, which in turn requires the calculation of the conduction bands for many $\mathbf{k}$ points. This last step is computationally very demanding due to the necessity of inverting large matrices. Moreover, this approach is limited to local pseudopotentials.

More recently, a method has been presented which combines the advantages of the two approaches mentioned above. Within density-functional perturbation

theory[12,13] (DFPT) the linear density response of the system to an external perturbation is calculated self-consistently via the solution of a set of equations which involve as known terms only quantities related to the unperturbed crystal with the atoms in their undisplaced configuration. Therefore, there is no need of using large supercells or inverting large matrices.

The present work displays the results of the *ab initio* calculation of lattice dynamical properties of diamond within the DFPT. We have calculated phonon dispersion curves along several high-symmetry directions in the Brillouin zone of the crystal. Our results are shown to be in well agreement with neutron[3] and synchrotron[4] scattering experiments. Furthermore, we predict phonon eigenvectors along the [111] and [100] directions, for which no experimental data are available. The internal-strain parameter is evaluated with different procedures. Finally, we calculate the thermal expansion coefficient of diamond within the quasiharmonic approximation (QHA). The agreement with experimental data is good; nevertheless, the relevance of terms in the phonon-phonon interaction beyond QHA is displayed in the high-temperature limit. As a by-product of the calculation we have obtained complete dispersion curves for the mode Grüneisen parameters.

The paper is organized as follows. In Sec. II we give a brief description of the employed method and some definitions concerning the physical quantities we have calculated. Then, the results of our calculation are presented and discussed in Sec. III. Finally, we draw some conclusions in Sec. IV.

II. THEORETICAL FRAMEWORK

A. Method

1. Basics

The harmonic lattice dynamics of a perfect crystal can be derived within the framework of the static linear-response theory.[7] In fact, the lattice distortion corresponding to a given phonon can be considered as a static perturbation acting on the electrons of the crystal. From the Hellmann-Feynman (HF) theorem[14] it can be shown that the linear electron-density response due to an external static perturbation yields the correct energy up to second order in the perturbation (up to third order, indeed, as shown in Ref. 15). For an external potential V_λ acting on the electrons (assumed local for simplicity) which depends continuously on a set of parameters $\lambda \equiv \{\lambda_i\}$ (e.g., the atomic coordinates), one obtains from the HF theorem the following expression for the second derivatives of the ground-state energy:[13]

$$\frac{\partial^2 \mathcal{E}_\lambda}{\partial\lambda_i \partial\lambda_j} = \int \left[\frac{\partial n_\lambda(\mathbf{r})}{\partial\lambda_j} \frac{\partial V_\lambda(\mathbf{r})}{\partial\lambda_i} + n_0(\mathbf{r}) \frac{\partial^2 V_\lambda(\mathbf{r})}{\partial\lambda_i \partial\lambda_j} \right] d^3r , \quad (1)$$

where $n_\lambda(\mathbf{r})$ is the electron density corresponding to the potential V_λ and the derivatives are calculated at $\lambda = 0$.

The linear electron-density response can be found, in principle, by solving the Schrödinger equation of the many-electron system. However, because of the huge number of electronic degrees of freedom, this procedure is not directly workable. Within density-functional theory (DFT), the ground-state electron density $n(\mathbf{r})$ is determined by finding the minimum of the functional representing the total energy of the crystal,[16]

$$\mathcal{E}[n] = T_0[n] + \int V_{\text{ion}}(\mathbf{r})\, d^3r + \int \frac{n(\mathbf{r})\, n(\mathbf{r}')}{|\mathbf{r} - \mathbf{r}'|}\, d^3r\, d^3r' + E_{\text{xc}}[n] + E_{\text{ion-ion}} , \quad (2)$$

where $T_0[n(\mathbf{r})]$ is the kinetic energy of a noninteracting electron gas of density $n(\mathbf{r})$ and $E_{\text{ion-ion}}$ is the contribution due to ion-ion interaction which is usually represented in terms of Ewald sums.[17] The unknown exchange-correlation energy $E_{\text{xc}}[n(\mathbf{r})]$ must be evaluated within some approximate scheme. The most widely used approximation is the so-called local-density approximation (LDA), in which the exchange-correlation energy density is approximated by the corresponding expression of the homogeneous electron gas, $\epsilon_{\text{xc}}(n(\mathbf{r}))$, evaluated at the local density of the actual inhomogeneous system,

$$E_{\text{xc}}^{\text{LDA}}[n(\mathbf{r})] = \int \epsilon_{\text{xc}}(n(\mathbf{r}))\, n(\mathbf{r})\, d^3r . \quad (3)$$

Therefore, the ground-state density is found by solving self-consistently the set of the Kohn-Sham one-particle equations[18] (atomic units are used throughout this paper)

$$\left(-\frac{1}{2}\nabla^2 + V_{\text{SCF}}(\mathbf{r}) \right) \phi_i(\mathbf{r}) = \epsilon_i\, \phi_i(\mathbf{r}) , \quad (4a)$$

$$V_{\text{SCF}}(\mathbf{r}) = V_{\text{ion}}(\mathbf{r}) + \int \frac{n(\mathbf{r}')}{|\mathbf{r} - \mathbf{r}'|}\, d^3r' + \frac{\delta E_{\text{xc}}[n]}{\delta n(\mathbf{r})} , \quad (4b)$$

$$n(\mathbf{r}) = \sum_i |\phi_i(\mathbf{r})|^2\, \Theta(\epsilon_F - \epsilon_i) . \quad (4c)$$

Here, the one-body self-consistent potential V_{SCF} consists of the external (ionic) potential acting on the electrons and of the effective electron-electron potential (Hartree and exchange-correlation potential), and ϵ_F is the Fermi energy which is fixed by the total number of electrons. Once the problem is solved for the unperturbed system the density response $\Delta n(\mathbf{r})$ can be found using first-order perturbation theory.[13,15] To linear order, a periodic perturbation ΔV_{ion} modifies the self-consistent potential V_{SCF} by a contribution ΔV_{SCF}. Then, linearization of Eqs. (4) yields a set of equations

$$\left(-\frac{1}{2}\nabla^2 + V_{\text{SCF}}(\mathbf{r}) - \epsilon_i \right) \Delta\phi_i(\mathbf{r}) = -[\, \Delta V_{\text{SCF}}(\mathbf{r}) - \langle \phi_i(\mathbf{r}) | \Delta V_{\text{SCF}}(\mathbf{r}) | \phi_i(\mathbf{r}) \rangle\,] \phi_i(\mathbf{r}) , \quad (5a)$$

$$\Delta V_{\rm SCF}(\mathbf{r}) = \Delta V_{\rm ion}(\mathbf{r}) + \int \frac{\Delta n(\mathbf{r}')}{|\mathbf{r}-\mathbf{r}'|}\, d^3r' + \Delta n(\mathbf{r}) \left[\frac{d\mu_{\rm xc}(\mathbf{r})}{dn}\right]_{n_0}, \tag{5b}$$

$$\mu_{\rm xc}(\mathbf{r}) = \frac{\delta E_{\rm xc}[n]}{\delta n(\mathbf{r})}, \qquad \Delta n(\mathbf{r}) = 2\,{\rm Re}\sum_i \phi_i^*(\mathbf{r})\,\Delta\phi_i(\mathbf{r})\,\Theta(\epsilon_F - \epsilon_i), \tag{5c}$$

which has to be solved self-consistently. It should be pointed out that, to linear order, the response has the same periodicity as the perturbation itself (given by the wave vector $\mathbf{q}$). As a final remark, one can observe that because of the similar structure of both the sets of Eqs. (4) and (5) the computational effort for solving them is of the same order.[12,13]

2. *Computational details*

The plane-wave pseudopotential method[19] is used to solve Eqs. (4) and (5). The dimension of the plane-wave basis set at a given $\mathbf{k}$ point in the first Brillouin zone is fixed through the condition

$$\tfrac{1}{2}(\mathbf{k}+\mathbf{G})^2 \le E_{\rm cut}, \tag{6}$$

where $\mathbf{G}$ is a reciprocal-lattice vector and $E_{\rm cut}$ is a kinetic-energy cutoff. Values of $E_{\rm cut}$ ranging from 55 Ry to 85 Ry were used to ensure convergence of the calculated quantities. Norm-conserving pseudopotentials for carbon have been generated following a scheme proposed by von Barth and Car.[20] For the expression of the LDA exchange-correlation energy we used the parametrization given in Ref. 21. The calculation of integrals over the BZ has been performed using ten Chadi-Cohen special points[22] in the irreducible wedge of the BZ. Further computational details have been already presented elsewhere.[13]

B. Harmonic properties

The calculation of phonon frequencies $\omega(\mathbf{q})$ and eigenvectors $\boldsymbol{u}_\kappa(\mathbf{q})$ requires the solution of the eigenvalue problem

$$\sum_{\kappa'} \boldsymbol{D}_{\kappa\kappa'}(\mathbf{q})\,\boldsymbol{u}_{\kappa'}(\mathbf{q}) = \omega^2(\mathbf{q})\,\boldsymbol{u}_\kappa(\mathbf{q}), \tag{7}$$

for the dynamical matrix with elements

$$D_{\alpha\kappa,\beta\kappa'}(\mathbf{q}) = \frac{1}{\sqrt{M_\kappa M_{\kappa'}}} \sum_{\mathbf{R}} C_{\alpha\kappa,\beta\kappa'}(\mathbf{R})\, e^{-i\mathbf{q}\cdot\mathbf{R}}, \tag{8}$$

where M_κ is the ionic mass of the κth atom, $\mathbf{R}$ is a Bravais lattice vector, and the *interatomic force constants* $C_{\alpha\kappa,\beta\kappa'}(\mathbf{R})$ are defined by the second derivatives of the total energy $\mathcal{E}$ of the crystal with respect to atomic displacements,

$$C_{\alpha\kappa,\beta\kappa'}(\mathbf{R}-\mathbf{R}') = \frac{\partial^2 \mathcal{E}}{\partial u_{\alpha\kappa}(\mathbf{R}) \partial u_{\beta\kappa'}(\mathbf{R}')}. \tag{9}$$

The force constants $\boldsymbol{C}_{\kappa\kappa'}(\mathbf{R})$ can be separated in an ionic and an electronic part

$$C_{\alpha\kappa,\beta\kappa'}(\mathbf{R}) = C^{\rm el}_{\alpha\kappa,\beta\kappa'}(\mathbf{R}) + C^{\rm ion}_{\alpha\kappa,\beta\kappa'}(\mathbf{R}), \tag{10}$$

where the ionic contribution can be easily calculated in terms of the second derivatives of the Ewald sums.[13] On the other hand, the electronic contribution to the force-constant matrix can be calculated—using the perturbation theory described in the previous section—from the response of the system to the atomic displacements $\{\mathbf{u}_\kappa(\mathbf{R})\}$. Therefore phonon frequencies and vibrational eigenvectors can be calculated at *any* wave vector $\mathbf{q}$ in the BZ of the crystal. Generally, no relation will hold between the phonon eigenvectors $\boldsymbol{u}_\kappa(\mathbf{q})$ defined by Eq. (7) and the wave vector $\mathbf{q}$. However, for wave vectors along high-symmetry lines such as the [111] or [100] direction, vibrational modes can be distinguished according to their purely transverse or longitudinal character. In such cases for crystals with the diamond structure the eigenvector of the dynamical matrix at the point $\mathbf{q}$ belonging to the jth branch can be written in the form[23]

$$\begin{aligned} \boldsymbol{u}_1^j(\mathbf{q}) &= \pm\frac{1}{\sqrt{2}}\,\mathbf{e}_j, \\ \boldsymbol{u}_2^j(\mathbf{q}) &= \frac{1}{\sqrt{2}}\,\exp[i\phi_j(\mathbf{q})]\,\mathbf{e}_j, \end{aligned} \tag{11}$$

where $\mathbf{e}_j$ is a real longitudinal ($j = L$) or transverse ($j = T$) unit vector (i.e., $\mathbf{e}_j \cdot \mathbf{e}_j = 1$), and we have defined the phase function $\phi_j(\mathbf{q})$ in such a way that it vanishes at $\mathbf{q} = 0$, so that the plus sign holds for acoustic modes, the minus for the optical ones.

From the knowledge of phonon eigenvectors one can extract information about the internal-strain properties of the crystal. The *internal-strain* tensor $\boldsymbol{\Delta}(\kappa)$ is defined as the proportionality constant between the sublattice displacement $\mathbf{d}(\kappa)$ and the macroscopic strain $\boldsymbol{\eta}$ applied to the crystal,

$$\mathbf{d}_\alpha(\kappa) = -\sum_{\beta\nu} \boldsymbol{\Delta}_{\alpha\beta\nu}(\kappa)\,\eta_{\beta\nu}. \tag{12}$$

In the diamond structure, symmetry requires that $\boldsymbol{\Delta}$ have only one independent component,

$$\boldsymbol{\Delta}_{\alpha\beta\nu}(1) = -\boldsymbol{\Delta}_{\alpha\beta\nu}(2) = -\zeta\,\frac{a}{4}\,|\epsilon_{\alpha\beta\nu}|, \tag{13}$$

where ζ is the so called internal-strain parameter and $\epsilon_{\alpha\beta\nu}$ is the fully antisymmetric Levi-Civita tensor. The internal-strain parameter can be obtained from the dependence of the longitudinal phase function ϕ_L upon $\mathbf{q}$

for $\mathbf{q} \to 0$.[23] Let $\mathbf{q} \equiv (2\pi/a)(\xi,\xi,\xi)$ be a wave vector along the [111] direction; then, one has

$$\zeta = \frac{3}{2} - \frac{1}{\pi}\left(\frac{\partial \phi_L(\xi)}{\partial \xi}\right)_{\xi=0} . \tag{14}$$

Furthermore, other equivalent phenomenologic expressions for the internal-strain tensor can be obtained[24] in terms of derivatives of the force $\mathbf{F}_\kappa$ acting on the atoms and of the macroscopic stress tensor $\boldsymbol{\sigma}$,

$$\mu\,\omega_{\mathrm{TO}}^2(\Gamma)\,\boldsymbol{\Delta}_{\alpha\nu\tau}(\kappa) = \left(\frac{\partial \mathbf{F}_{\alpha\kappa}}{\partial \boldsymbol{\eta}_{\nu\tau}}\right)_{\mathbf{u}=0} = \frac{V_0}{N}\left(\frac{\partial \boldsymbol{\sigma}_{\nu\tau}}{\partial \mathbf{u}_{\alpha\kappa}}\right)_{\eta=0} , \tag{15}$$

where V_0 is the equilibrium crystal volume, N the number of unit cells of the lattice, $\omega_{\mathrm{TO}}(\Gamma)$ the transverse optic frequency at $\mathbf{q} = 0$, and μ is the reduced mass. Using the previous equation, we obtain two other equivalent ways for calculating ζ, the former from the derivative of the force acting on the atom κ with respect to the strain at vanishing displacements $\mathbf{u}$ from the equilibrium position and the latter from the derivative of the stress with respect to the atomic displacement at zero strain.

C. Anharmonic properties

The equilibrium lattice parameter of a crystal at finite temperature in the absence of any applied pressure is obtained by minimizing the Helmholtz free energy,

$$F(T,V) = U(T,V) - T\,S(T,V) , \tag{16}$$

where U is the internal energy and S the entropy. In the harmonic approximation, phonon-phonon interactions are completely neglected. As a consequence, the vibrational part of the Helmholtz free energy and in particular the phonon frequencies do not depend on the volume, and no thermal expansion is possible for a purely harmonic crystal. A simple approach which accounts for anharmonics effects is the so-called quasiharmonic approximation (QHA), in which the free energy is written in the same way as in the harmonic approximation, but allowing for the dependence of the frequencies on the volume,

$$F^{\mathrm{QHA}}(T,V) = U_0(V) + F_{\mathrm{vib}}^{\mathrm{QHA}}(T,V) , \tag{17}$$

where $U_0(V)$ is the internal energy at $T = 0$ and

$$F_{\mathrm{vib}}^{\mathrm{QHA}}(T,V) = k_B T \sum_{\mathbf{q},j} \ln\left[1 - \exp\left(-\frac{\hbar\omega_j(\mathbf{q},V)}{k_B T}\right)\right] \tag{18}$$

Within this approximation the thermal expansion coefficient $\alpha(T)$ can be obtained as[25,26]

$$\alpha(T) = \frac{1}{3V}\frac{\partial V}{\partial T} \approx \frac{1}{B_0}\sum_{\mathbf{q},j}\gamma_j(\mathbf{q})\,c_{vj}(\mathbf{q},T) , \tag{19}$$

where B_0 is the bulk modulus at equilibrium, $c_{vj}(\mathbf{q},T)$ is the contribution of the mode $\mathbf{q}\,j$ to the specific heat at constant volume, and $\gamma_j(\mathbf{q})$ is the mode Grüneisen parameter defined by

$$\gamma_j(\mathbf{q}) = -\frac{V_0}{\omega_j(\mathbf{q},V_0)}\left(\frac{\partial \omega_j(\mathbf{q},V)}{\partial V}\right)_{V=V_0} . \tag{20}$$

III. RESULTS

A. Equilibrium properties

The equilibrium lattice structure at $T = 0$ is determined by minimizing the crystal total energy $\mathcal{E}(V)$ as a function of the structural parameters. In the case of the diamond structure the only relevant parameter is the lattice constant a. To the purpose of minimizing $\mathcal{E}(V)$ the values of the total energy calculated at a fixed kinetic-energy cutoff for different lattice constants have been fitted to Murnaghan's equation of state,[27]

$$\mathcal{E}(V) = \frac{V_0 B_0}{B_0'}\left[\frac{1}{B_0' - 1}\left(\frac{V_0}{V}\right)^{B_0'-1} + \frac{V}{V_0}\right] + \mathrm{const} , \tag{21}$$

where B_0' is the derivative of the bulk modulus with respect to the pressure. The fitting procedure has been repeated for kinetic-energy cutoff up to 85 Ry. The converged results (up to the figures quoted) for the equilibrium parameters are shown in Table I and compared with the corresponding experimental values; the obtained agreement is very good. Also the calculated valence charge density (see Fig. 1) is in good agreement with previous theoretical calculations.[2,10] It is worthwhile to mention the relevant role of the p orbitals of carbon in the formation of the characteristic double-hump feature of the electron density along the bonds.

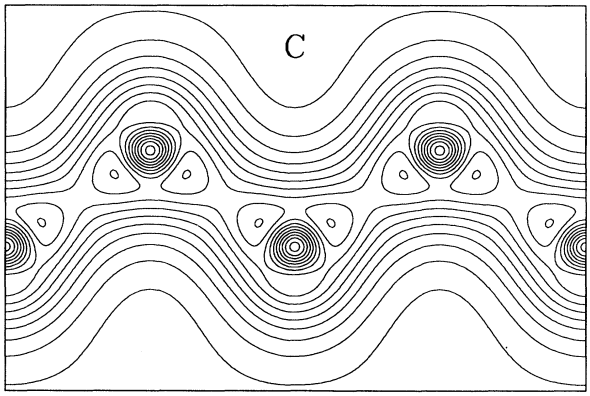

FIG. 1. Calculated valence charge density in the (110) plane of diamond. The charge density is in units of electrons per Å^3. The contour interval is 0.2 e/Å^3. The maximum of the charge along the bonds is 2.0 e/Å^3.

TABLE I. Equilibrium lattice parameter a (a.u.), bulk modulus B_0 (Mbar), pressure derivative of the bulk modulus B_0', and static (with clamped nuclei) dielectric constant ϵ_∞.

	a	B_0	B_0'	ϵ_∞
Theor.	6.67	4.73	3.5	5.72
Expt.	6.74[a]	4.52[a]	4.0[b]	5.70[a]

[a]Ref. 36.
[b]Ref. 37.

B. Phonon dispersion curves

Our results for the bulk phonon dispersion curves of diamond along several symmetry lines together with the corresponding density of states (DOS) are displayed in Fig. 2. Some numerical values at the high-symmetry points Γ, X, and L are also reported in Table II. A kinetic-energy cutoff of 55 Ry ensures a convergence of the calculated frequencies with an accuracy of 1–2%. The agreement with the available neutron[3] and synchrotron[4] scattering data is very good. Most of tetrahedral semiconductors show a peculiar flatness of the transverse acoustic (TA) modes over a large portion of the BZ which causes the structures of the density of states in the acoustic frequencies region.[13] The case of diamond is quite different: The TA branches are no longer flat; the sharp features in the corresponding region of the phonon density of states are thus lacking. Another very interesting peculiarity has been found in the phonon spectrum of diamond: The maximum of the optical branches is not at the zone center as it is the case of silicon and germanium.[13] Along the different high-symmetry directions of diamond a maximum at $\mathbf{q} \neq 0$ has been found. A comparative analysis of the interatomic force constants in diamond and in silicon (where no overbending is present) reveals that a necessary condition to have a minimum of the uppermost branch at the Γ point is to have sufficiently large interatomic force constants between second-nearest neighbors. The existence of the overbending causes a sharp peak as well in the phonon density of states above the Γ point optical frequency as in the second-order Raman spectrum.[28] Experimental evidence of this sharp peak has been found in the second-order Raman spectrum of diamond.[29]

TABLE II. Phonon frequencies of diamond at the high-symmetry points Γ, X, and L. The values are expressed in cm^{-1}.

	Γ_O	X_{TA}	X_{TO}	X_L	L_{TA}	L_{LA}	L_{TO}	L_{LO}
Theor.	1324	800	1094	1228	561	1080	1231	1275
Expt.[a]	1331	803	1077	1194	552	1035	1210	1242

[a]Ref. 3.

C. Phonon eigenvectors

We have calculated the phase function $\phi(\mathbf{q})$ defined in Eq. (11) for phonon eigenvectors along the [100] and [111] direction. Our results are depicted in Figs. 3(a) and 3(b). Also in this case the behavior of the phase function of diamond is peculiar with respect to the general case of most of the tetrahedral semiconductors such as Si, GaAs, etc.[24] In particular, the main difference concerns the longitudinal eigenvectors along the Λ direction. For a direct comparison we also report in Fig. 3(b) the phase function for longitudinal-acoustic modes of silicon which is typical for the rest of the tetrahedral semiconductors. At the L point the longitudinal phase vanishes in the case of silicon, whereas in diamond it is equal to π leading to an opposite sign in the atomic displacements of the atoms in the unit cell. This may be erroneously considered in disagreement with the acoustic or optical character of the eigenmodes. In fact, a real distinction between acoustic and optical modes holds only at the Γ point. Because of symmetry reasons, the eigenvectors at the L point can be chosen real so that both the values 0 and π are allowed for the phase factor. Actually, the unit (super)cell associated with a phonon at the L point is twice as large as

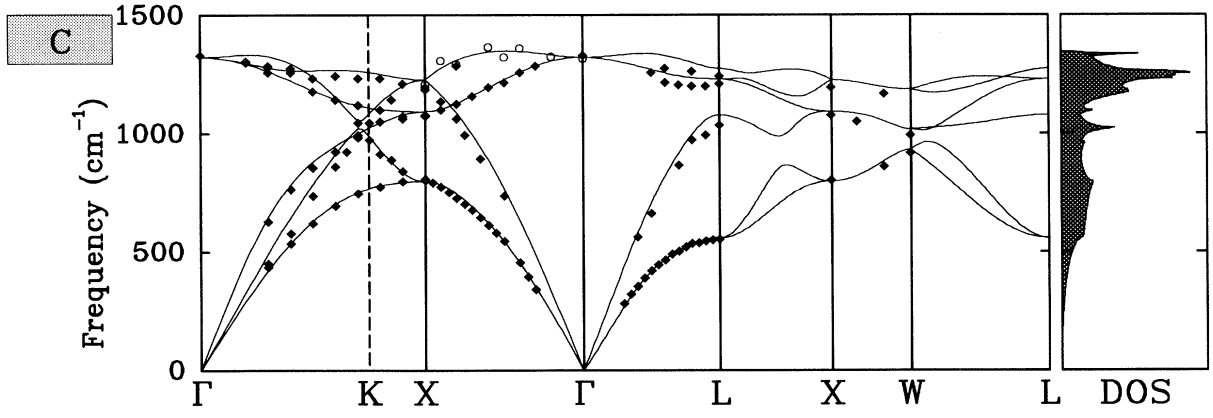

FIG. 2. Calculated phonon dispersion curves and density of states (DOS) of diamond. Experimental neutron-scattering data are denoted by diamonds (from Ref. 3). Some experimental data from synchrotron scattering (open circles, from Ref. 4) are also displayed for the uppermost branch in the [100] direction.

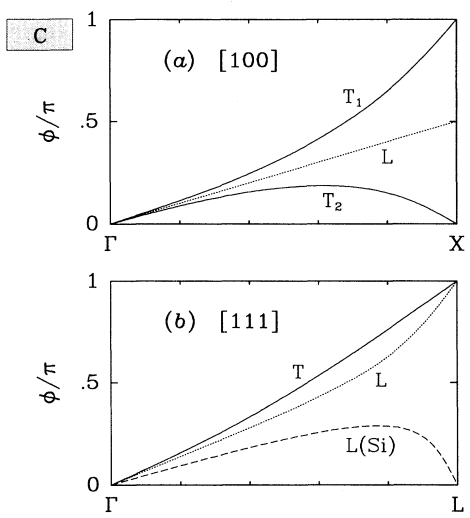

FIG. 3. (a) Theoretical eigenvector phase function $\phi(\mathbf{q})$ of diamond along the [100] direction for transverse (solid lines) and longitudinal (dotted line) modes. The transverse mode T_1 (T_2) is polarized along the $\bar{y}z$ (yz) direction, the symmetry of the crystal imposes that $\phi(q,0,0;T_1)+\phi(q,0,0;T_2) = q/(2a)$. The phase function for longitudinal modes is entirely determined by symmetry as $\phi_L(q,0,0) = q/(4a)$. (b) Same as (a) but for the [111] direction. For comparison we report also the longitudinal phase function of silicon (dashed line) along the same direction (from Ref. 24).

the unit cell of the unperturbed crystal, and the eigenvectors have opposite phases in the two unit cells. Thus, the difference between the two longitudinal modes is that the $\phi = \pi$ mode involves the stretching of the [111] bond, whereas the other bonds remain unchanged (*bond-stretching* mode); on the contrary, in the $\phi = 0$ mode the length of the [111] bond remains unchanged and the angles between the other three bonds are changed (*bond-bending* mode). In diamond the bond-bending mode has a higher frequency than the bond-stretching one. The converse holds for the other semiconductors.[24] This particular behavior shows that in diamond the ratio between the force constants associated with the bond-bending and those with bond-stretching displacements is significantly larger than in the other cases. This interpretation agrees with results extracted from the force constants in the Keating model[30] fitted to experimental data.

D. Internal-strain parameter

We have calculated the internal-strain parameter of diamond with all of the three methods we have previously described [see Eqs. (14) and (15)]. A first estimate was made starting from the phase function in the [111] direction. The eigenvectors of the dynamical matrix have been calculated using the *interplanar* force constants along the Λ direction. Then, we calculated the stress tensor with the crystal in the undistorted structure (i.e., at zero macroscopic strain), with one of the two atoms in the unit cell displaced in the [111] direction. The amplitude of the displacement was chosen in such a way as to guarantee linearity without affecting the results with numerical noise. Finally, the forces acting on the atoms at the equilibrium in a strained structure along the Λ direction have been calculated. A kinetic-energy cutoff $E_{\rm cut} = 75$ Ry has been used to achieve an accuracy of 5% for all of the methods. The results obtained with the three methods are shown in Table III in comparison with the available experimental data. Our results agree well with both the experimental value and the value of $\xi = 0.108$ obtained by previous *ab initio* calculations.[9] At variance with the others, the slightly smaller value obtained from the linearization of the forces expresses the sensitivity of finite-difference methods to the shape (and symmetry) of the used unit cell.

TABLE III. Internal-strain parameter of diamond. (a) Value derived from the slope of the phase function $\phi(\mathbf{q})$ at $\mathbf{q} = 0$. (b) Value obtained from the linearization of the stress vs the displacement. (c) Value obtained from the linearization of the forces vs the strain.

	(a)	(b)	(c)	Expt.
ξ	0.12	0.11	0.09	0.13[a]

[a]Ref. 38.

E. Grüneisen constants and thermal expansion

We have performed the calculation of the interatomic force constants at different lattice parameters in the neighborhood of the equilibrium value. Then, the derivatives of the frequencies have been evaluated numerically using quadratic interpolation. Analogously to the case of the phonon frequencies, we have obtained the dispersion curves of the mode Grüneisen parameters along several symmetry directions using Eq. (20). These results are shown and compared with available experimental data in Fig. 4. Because of the vanishing acoustic frequencies at the Γ point, the dispersions of the acoustic branches are discontinuous at the BZ center, and the value of the Grüneisen parameters in the limit $\mathbf{q} \to 0$ depends, for such modes, on the direction of $\mathbf{q}$. At variance with results for Si and Ge,[26] the mode Grüneisen parameters of diamond are found to be positive throughout the BZ for *all* branches. Along the [110] direction sharp features near the K point are found in the mode Grüneisen dispersion curves of the longitudinal-optical and z-polarized transverse-acoustic branches. These features are related to the large absolute value of the second derivative of the corresponding frequency dispersion curves along the [110] direction, evaluated at the branch minimum (for the optical one) or maximum (for the acoustic one).

The thermal expansion coefficient of diamond has then been evaluated following Eq. (19). The sum over phonon modes has been performed using 182 points in the irreducible wedge of the BZ; further increase of the number of $\mathbf{q}$ points does not change significantly our results. The obtained temperature dependence of the coefficient

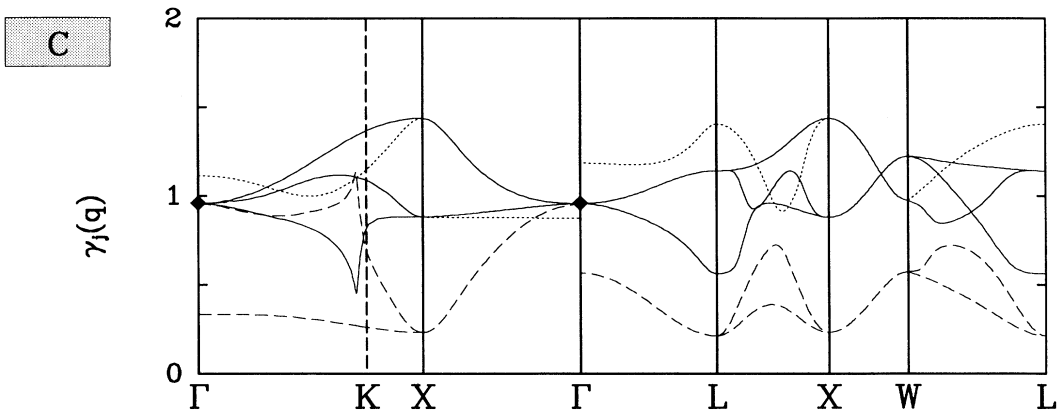

FIG. 4. Calculated dispersion curves of the mode Grüneisen parameters $\gamma_j(\mathbf{q})$ of diamond. Dashed lines correspond to transverse acoustic modes, dotted lines to longitudinal acoustic modes, and solid lines to optical modes. Experimental data are denoted by diamonds (from Ref. 35).

$\alpha(T)$ for diamond is displayed in Fig. 5. At variance with other group-IV and III-V crystals there is no temperature range with a negative thermal expansion. The anomalies in the thermal expansion at low temperatures of tetrahedral semiconductors are due to the negative values of the transverse-acoustic-mode Grüneisen parameters at the BZ boundaries.[26,31] Concerning the sign of the Grüneisen parameters for these modes, it can be shown[31] that positive values are obtained only when contribution due to angular forces are dominant with respect to those of central forces. As already remarked, the mode Grüneisen parameters of these branches are positive in diamond, leading to non-negative $\alpha(T)$.

In the QHA at temperatures of the order of the Debye temperature all the phonon modes in the crystal are excited and $\alpha(T)$ displays a tendency to saturate to a constant value. The residual dependence of α upon T is due to the dependence of the Grüneisen parameters upon the volume which is determined by higher-order anharmonic effects.

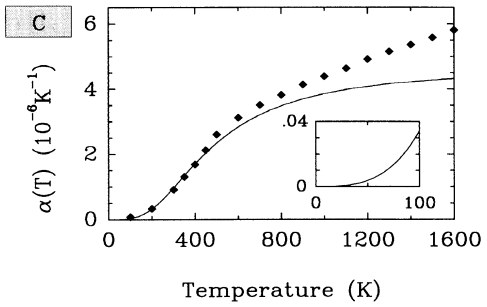

FIG. 5. Thermal expansion coefficient $\alpha(T)$ of diamond as a function of temperature. The inset shows the details at low temperatures. Experimental data are denoted by diamonds (from Ref. 5).

IV. CONCLUSIONS

The lattice dynamics of diamond shows many interesting features which are related to the particular nature of the constituent carbon atoms. Uniquely among the group-IV elements, carbon has no p electrons in the core. Its valence configuration is $2s^2 2p^2$ and the atomic orbitals in the tetrahedral structure of the diamond crystal are strongly hybridized in an sp^3 configuration. Even if this kind of hybridization is present in the other tetrahedral elemental semiconductors, the absence of p core states causes a particular "rigidity" of the sp^3 configuration in diamond. Such a strength of the hybridization drastically affects those properties of the crystal which are connected to the variation of the angles formed by adjacent bonds between the atoms. In fact, angular interatomic force constants assume particularly large values in diamond in comparison with the other tetrahedral compounds. These facts are shown to be responsible for most of the peculiarity of the lattice dynamical properties of diamond.

We have shown that parameter-free calculations can achieve an accurate description of static and vibrational properties of diamond. The calculated equilibrium parameters are comparable with the experimental results within a few percent. The phonon frequencies obtained from our *ab initio* calculations are in good agreement with available experimental data and, furthermore, give a reliable prediction for the experimentally unknown features of the phonon spectrum of diamond, e.g., the overbending which is present in the uppermost branch around the Γ point. Moreover, the phase function of the eigenvectors of the diamond crystal has been shown to be different from that of the other group-IV semiconductors. Whereas at the L point in the BZ a bond-bending character is found in the longitudinal-acoustic mode of diamond, in the other cases it is a bond-stretching mode. We have also shown that, in agreement with experimental results, there is no negative thermal expansion in diamond,

in contrast to Si, Ge, or α-Sn. This behavior reflects the fact that for diamond all mode Grüneisen parameters are positive in the whole BZ.

Finally, one should remark that the convergence of the vibrational frequencies requires a very large kinetic-energy cutoff (55 Ry in the best case). In view of further applications to more complex systems based on carbon, one should be addressed to the very recent developments within the field of soft norm-conserving pseudopotentials.[32,33] Preliminary calculations have been carried out for graphite[34] using soft norm-conserving pseudopotentials[32]. In this way the size of the plane-wave basis set can be cut down by one-third—indeed a kinetic-energy cutoff of only 40 Ry is sufficient for calculating converged frequencies—allowing a strong reduction of the computational effort.

ACKNOWLEDGMENTS

This work has been cosponsored by the Italian *Consiglio Nazionale delle Ricerche* under Grant No. 91.00943.PF69, by the European Research Office of the U.S. Army under Grant No. DAJA 45-89-C-0025, and by the *Deutsche Forschungsgemeinschaft* (Graduierten-Kolleg: Komplexität in Festkörpern) under Contract No. SCHR123/8.

[1] C. Kittel, *Introduction to Solid State Physics*, 5th ed. (Wiley, New York, 1976).
[2] M. T. Yin and M. L. Cohen, Phys. Rev. B **24**, 6121 (1981); G. B. Bachelet, H. S. Greenside, G. A. Baraff, and M. Schlüter, *ibid.* **24**, 4745 (1981); P. E. Camp, V. E. Van Doren, and J. T. Devreese, *ibid.* **34**, 1314 (1986).
[3] J. L. Warren, J. L. Yarnell, G. Dolling, and R. A. Cowley, Phys. Rev. **158**, 805 (1967).
[4] E. Burkel, *Inelastic Scattering of X Rays with Very High Energy Resolution*, Vol. 125 of *Springer Tracts in Modern Physics* (Springer, Berlin, 1991) (especially pp. 61–64).
[5] G. A. Slack and S. F. Bartram, J. Appl. Phys. **46**, 89 (1975).
[6] H. Wendel and R. M. Martin, Phys. Rev. B **19**, 5251 (1979); K. Kunc and R. M. Martin, Phys. Rev. Lett. **48**, 406 (1982); M. T. Yin and M. L. Cohen, Phys. Rev. B **26**, 3259 (1982).
[7] L. J. Sham, Phys. Rev. **188**, 1431 (1969); R. Pick, M. H. Cohen, and R. M. Martin, *ibid.* **1**, 910 (1970).
[8] J. R. Chelikowsky and S. G. Louie, Phys. Rev. B **29**, 3470 (1984).
[9] O. H. Nielsen, Phys. Rev. B **34**, 5808 (1986).
[10] A. Fukumoto, Phys. Rev. B **42**, 7462 (1990).
[11] D. Vanderbilt, S. G. Louie, and M. L. Cohen, Phys. Rev. Lett. **53**, 1477 (1984); D. Vanderbilt, S. G. Louie, and M. L. Cohen, Phys. Rev. B **33**, 8740 (1986).
[12] S. Baroni, P. Giannozzi, and A. Testa, Phys. Rev. Lett. **58**, 1861 (1987); N. E. Zein, Fiz. Tverd. Tela **26**, 3028 (1984) [Sov. Phys. Solid State **26**, 1825 (1984)].
[13] P. Giannozzi, S. de Gironcoli, P. Pavone, and S. Baroni, Phys. Rev. B **43**, 7231 (1991).
[14] H. Hellmann, *Einführung in die Quantenchemie* (Deuticke, Leipzig, 1937); R. P. Feynman, Phys. Rev. **56**, 340 (1939).
[15] X. Gonze and J. P. Vigneron, Phys. Rev. B **39**, 13120 (1989).
[16] P. Hohenberg and W. Kohn, Phys. Rev. **136**, B864 (1964).
[17] J. Ihm, A. Zunger, and M. L. Cohen, J. Phys. C **12**, 4409 (1979).
[18] W. Kohn and L. J. Sham, Phys. Rev. **140**, A1133 (1965); L. J. Sham and W. Kohn, *ibid.* **145**, B561 (1966).
[19] For an excellent review, see W. E. Pickett, Comput. Phys. Rep. **9**, 115 (1989).
[20] U. von Barth and R. Car (unpublished). This procedure consists in practice of a fitting minimization of the squared differences between the atomic all-electron and pseudoeigenvalues and eigenfunctions (outside the core sphere) as a function of a few parameters upon which the pseudopotential depends.
[21] J. Perdew and A. Zunger, Phys. Rev. B **23**, 5048 (1981).
[22] D. J. Chadi and M. L. Cohen, Phys. Rev. B **8**, 5747 (1981).
[23] D. Strauch, A. P. Mayer, and B. Dorner, Z. Phys. B **78**, 405 (1990).
[24] P. Pavone, D. Strauch, and S. Baroni (unpublished).
[25] T. H. K. Barron, J. G. Collins, and G. K. White, Adv. Phys. **29**, 609 (1980).
[26] P. Pavone and S. Baroni (unpublished).
[27] F. D. Murnaghan, Proc. Natl. Acad. Sci. USA **50**, 697 (1944).
[28] W. Windl, P. Pavone, K. Karch, O. Schütt, D. Strauch, P. Giannozzi, and S. Baroni, following paper, Phys. Rev. B **48**, 3164 (1993).
[29] S. A. Solin and A. K. Ramdas, Phys. Rev. B **1**, 1687 (1970); M. A. Washington and H. Z. Cummings, Phys. Rev. B **15**, 5840 (1977).
[30] R. M. Martin, Phys. Rev. B **1**, 4005 (1970).
[31] C. H. Xu, C. Z. Wang, C. T. Chan, and K. M. Ho, Phys. Rev. B **43**, 5024 (1991).
[32] N. Troullier and J. L. Martins, Phys. Rev. B **43**, 1993 (1991).
[33] D. Vanderbilt, Phys. Rev. B **41**, 7892 (1990).
[34] P. Pavone, K. Karch, O. Schütt, W. Windl, and D. Strauch (unpublished).
[35] B. B. Pate, I. Lindau, and W. E. Spicer, in *Proceedings of the 17th International Conference on the Physics of Semiconductors*, San Francisco, 1984, edited by J. D. Chadi and W. A. Harrison (Springer-Verlag, New York, 1985), p. 1181.
[36] *Physics of Group IV and III-V Compounds*, edited by O. Madelung, Landolt-Börnstein, New Series, Group III, Vol. 17a (Springer-Verlag, Berlin, 1982), p. 107.
[37] K. Geschneider, Jr., in *Solid State Physics*, edited by F. Seitz, D. Turnbull, and H. Ehrenreich (Academic, New York, 1964), Vol. 16, p. 275.
[38] C. S. G. Cousins, L. Gerward, J. Staun Olsen, and B. J. Sheldon, J. Phys. Condens. Matter **1**, 29 (1989).